

Which Interactions Dominate in Active Colloids?

Benno Liebchen^{1, a)} and Hartmut Löwen¹

Institut für Theoretische Physik II: Weiche Materie, Heinrich-Heine-Universität Düsseldorf, D-40225 Düsseldorf, Germany

(Dated: 28 February 2022)

Despite a mounting evidence that the same gradients which active colloids use for swimming, induce important cross-interactions (phoretic interaction), they are still ignored in most many-body descriptions, perhaps to avoid complexity and a zoo of unknown parameters. Here we derive a simple model, which reduces phoretic far-field interactions to a pair-interaction whose strength is mainly controlled by one genuine parameter (swimming speed). The model suggests that phoretic interactions are generically important for autophoretic colloids (unless effective screening of the phoretic fields is strong) and should dominate over hydrodynamic interactions for the typical case of half-coating and moderately nonuniform surface mobilities. Unlike standard minimal models, but in accordance with canonical experiments, our model generically predicts dynamic clustering in active colloids at low density. This suggests that dynamic clustering can emerge from the interplay of screened phoretic attractions and active diffusion.

I. INTRODUCTION

Since their first realization at the turn to the 21st century^{1,2}, active colloids³⁻⁵ have evolved from synthetic proof-of-principle microswimmers toward a versatile platform for designing functional devices. Now, they are used as microengines^{3,6-9} and cargo-carriers^{10,11}, aimed to deliver drugs towards cancer cells in the future, and spark a huge potential for the creation of new materials through nonequilibrium self-assembly¹²⁻¹⁹. These colloids self-propel by catalyzing a chemical reaction on part of their surface, resulting in a gradient which couples to the surrounding solvent and drives them forward. When many active colloids come together, they self-organize into spectacular patterns, which would be impossible in equilibrium and constitutes their potential for nonequilibrium self-assembly. A typical pattern, re-occurring in canonical experiments with active Janus colloids, are so-called living clusters which spontaneously emerge at remarkably low densities (area fraction 3 – 10%) and dynamically split up and reform as time proceeds^{12,22-24}. When trying to understand such collective behaviour in active colloids, we are facing complex setups of motile particles showing multiple competing interactions, such as steric, hydrodynamic and phoretic ones (the latter ones hinge on the cross-action of self-produced chemicals on other colloids).

Therefore, to reduce complexity and to allow for descriptions which are simple enough to promote our understanding of the colloids' collective behaviour, yet sufficiently realistic to represent typical experimental observations (such as dynamic clustering) we have to resolve the quest: which interactions dominate in active colloids? Presently, the most commonly considered models in the field, like the popular Active Brownian particle model^{25,26} and models involving hydrodynamic interactions^{27,28} neglect phoretic interactions altogether, perhaps to avoid complexity and unknown parameters which their description usually brings along. Conversely, recent experiments^{12,16,19,22}, simulations^{20,21}, and theories²⁹

suggest a crucial importance of phoretic interactions in various active colloids - which, after 15 years of research on active colloids, still leaves us with a conflict – calling for minimal models accounting for phoretic interactions.

Here, our aim is (i) to demonstrate that phoretic interactions are *generically* important in active colloids (unless for strong effective screening) and often seem to be the dominant far-field interaction, (ii) to derive a minimal description of these often neglected interactions, making it easier to account for them in future simulations and theories and (iii) to show that this minimal description is sufficient to predict dynamic clustering, as seen in experiments^{12,22-24} but not in standard minimal models of active colloids. More specifically, we derive the Active Attractive Alignment model (AAA model), providing a strongly simplified description of active colloids by reducing phoretic interactions to a simple pair interaction among the colloids. This allows to include them e.g. in Brownian dynamics simulations, rather than requiring hybrid particle-field descriptions and releases their modeling from the zoo of unknown parameters it usually involves³⁹⁻⁴⁴. Remarkably, our derivation shows that the strength of phoretic interactions is mainly controlled by one genuine parameter, the self-propulsion speed (or Péclet number), rather than involving many unknown parameters. This allows to compare the strength of phoretic interactions with hydrodynamic interactions. Our comparison suggest that phoretic interactions even dominate over hydrodynamic interactions for the common case of half-coated Janus colloids with a uniform or a moderately nonuniform surface mobility. Thus, as opposed to microswimmers moving by body-shape deformations^{27,30-38}, which are often dominated by hydrodynamic interactions, many active colloids seem to be rather dominated by phoretic interactions. Performing Brownian dynamics simulations we find that the AAA model generically predicts dynamic clustering at low density, in agreement with experiments^{12,22-24}, but as opposed to standard minimal models of active colloids.

Our approach should be broadly useful to model active colloids and to design active self-assembly^{16,19,45,46}. It can be used when the phoretic fields relax quasi-instantaneously, which should apply to the common case where phoretic interactions are attractive – in contrast repulsive phoretic interactions can lead to important delay effects requiring to explicitly

^{a)}liebchen@hhu.de

account for the time-evolution of phoretic fields²⁹.

II. PHORETIC MOTION IN EXTERNAL GRADIENTS

When exposed to a gradient in an imposed phoretic field c , which may represent e.g. a chemical concentration field, the temperature field or an electric potential, colloids move due to phoresis. Here, the gradients in c act on the fluid elements in the interfacial layer of the colloid and drive a localized solvent flow tangentially to the colloidal surface with a velocity, called slip velocity

$$\mathbf{v}_s(\mathbf{r}_s) = \mu(\mathbf{r}_s) \nabla_{\parallel} c(\mathbf{r}_s) \quad (1)$$

Here $\mu(\mathbf{r}_s)$ is the phoretic surface mobility, \mathbf{r}_s points to the colloidal surface (outer edge of interfacial layer) and $\nabla_{\parallel} c$ is the projection of the gradient of c onto the tangential plane of the colloid. The colloid moves opposite to the average surface slip with a velocity⁴⁷ $\mathbf{v} = \langle -\mathbf{v}_s(\mathbf{r}_s) \rangle$ where brackets represent the average over the colloidal surface. If the solvent slips asymmetrically over the colloidal surface, the colloid also rotates with a frequency⁴⁷ $\Omega = \frac{3}{2R} \langle \mathbf{v}_s(\mathbf{r}_s) \times \mathbf{n} \rangle$ where R, \mathbf{n} are the radius and the local surface normal of the colloid. Performing surface integrals, and focusing, from now on, on spherical Janus colloids with a catalytic hemisphere with surface mobility μ_C , and a mobility of μ_N on the neutral side, yields:

$$\mathbf{v}(\mathbf{r}) = -\frac{\mu_C + \mu_N}{3} \nabla c; \quad \Omega(\mathbf{r}) = \frac{3(\mu_N - \mu_C)}{8R} \mathbf{e} \times \nabla c \quad (2)$$

Here, we have neglected deformations of the field due to the presence of the Janus particle⁴⁸, evaluate c at the colloid center \mathbf{r} for simplicity, and have introduced the unit vector \mathbf{e} pointing from the neutral side to the catalytic cap.

III. SELF-PROPULSION

Autophoretic colloidal microswimmers, or active colloids, self-produce phoretic fields on part of their surface with a local surface production rate $\sigma(\mathbf{r}_s)$. In steady state, we can calculate the field produced by a colloid centered at the origin by solving

$$0 = D_c \nabla^2 c(\mathbf{r}) + \oint d\mathbf{r}_s \delta(\mathbf{r} - \mathbf{r}_s) \sigma(\mathbf{r}_s) - k_d c(\mathbf{r}) \quad (3)$$

where the integral is performed over the colloidal surface, D_c is the diffusion coefficient of the relevant phoretic field⁴⁹ and the sink term $-k_d c$ represents a minimal way to model an effective decay of the phoretic fields, leading to effective screening, which may result e.g. from bulk reactions²⁰ (including fuel recovery¹⁶) for chemicals and ions. While commonly neglected in the literature, Fig. 1G suggests that phoretic fields are effectively screened at least for some colloids, which influences phoretic interactions. (For self-thermophoretic swimmers, k_d might be zero if absorbing boundaries are absent.) Conversely, self-propulsion, i.e. the phoretic drift of a colloid

in its self-produced gradient, depends only on the phoretic field close to its surface, so that we can ignore the decay. Considering a Janus colloid producing chemicals with a local rate $\sigma = k_0/(2\pi R^2)$ on one hemisphere and $\sigma = 0$ on the other one, using Eqs. (1,3) for $k_d = 0$ and $\mathbf{v}_0 = \langle -\mathbf{v}_s(\mathbf{r}_s) \rangle$, we obtain^{7,50}

$$\mathbf{v}_0 = -\frac{k_0(\mu_N + \mu_C)}{16\pi R^2 D_c} \mathbf{e} \quad (4)$$

For symmetry reasons the considered Janus colloids do not show self-rotations.

IV. HOW STRONG ARE PHORETIC INTERACTIONS?

Besides leading to self-propulsion, the gradients produced by an autophoretic colloid also act in the interfacial layer of all other colloids. Here, they drive a solvent slip over the colloids' surfaces, which induce a phoretic translation and a rotation. Following Eqs. (1,2,4) a colloid at the origin causes a translation and rotation of a test Janus colloid at position \mathbf{r} with

$$\mathbf{v}_P(\mathbf{r}) = -v \frac{16\pi R^2 D_c v_0}{3k_0} \nabla c; \quad \Omega_P(\mathbf{r}) = \mu_r \frac{6\pi D_c R v_0}{k_0} \mathbf{p} \times \nabla c \quad (5)$$

where \mathbf{p} is the unit vector pointing from \mathbf{r} into the swimming direction of the test colloid. Here, $v = -1$ for swimmers moving with their catalytic cap ahead and $v = 1$ for cap-behind swimmers²⁹; we have further used $v_0 = |v_0|$ and have introduced the reduced surface mobility $\mu_r = (\mu_C - \mu_N)/(\mu_C + \mu_N)$. Now solving Eq. (3) in far-field (the integral reduces to $k_0 \delta(\mathbf{r})$), yields the phoretic field produced by the colloid at the origin

$$c(\mathbf{r}) \approx \frac{k_0 e^{-\kappa r}}{4\pi D_c r} \quad (6)$$

for $\kappa R/2 \ll 1$ and $r \gg R$, where $\kappa = \sqrt{k_d/D_c}$ is an effective inverse screening length and $\kappa = 0$ represents the unscreened case. (Note that our approach assumes that the phoretic field relaxes quasi-instantaneously to its steady state, which is a useful limit for attractive phoretic interactions on which we focus here, but can be dangerous at least for the repulsive case²⁹.) Finally combining Eqs. (5) and (6) yields, in leading order

$$\mathbf{v}_P(\mathbf{r}) = \frac{-4v_0 R^2 v}{3} \nabla \frac{e^{-\kappa r}}{r} \quad (7)$$

$$\Omega_P(\mathbf{r}) = \frac{3v_0 R \mu_r}{2} \mathbf{p} \times \nabla \frac{e^{-\kappa r}}{r} \quad (8)$$

Except for κ, μ_r which we will estimate below and $v = \pm 1$, the prefactors in Eqs. (7,8) only depend on the self-propulsion velocity and the colloidal radius, which are well known in experiments. We can further see from Eq. (7) that colloids at a typical distances of $\sim 5R$ with $R \sim 1\mu\text{m}$; $v_0 \sim 10\mu\text{m/s}$, approach each other (for $v = -1$) within a few seconds due to phoretic interactions (this is consistent with experiments,

e.g.^{12,16}). For colloids with $R = 1\mu\text{m}$, $v_0 \sim 10\mu\text{m/s}$, $|\mu_r| = 0.15$ ⁵¹, the alignment rate with the phoretic gradient produced by an adjacent colloid is $|\Omega| \sim 0.1/s$, i.e. for the attractive case ($v = -1$) colloids may approach each other due to phoretic translation before turning much. Thus, it is plausible that when forming dynamic clusters (see below), Janus colloids do not show much orientational order²⁴. Still, phoretic alignment should generally play a crucial role for the stability of the uniform phase^{29,52}, particularly when $|\mu_r| \sim 1$ as e.g. certain thermophoretic swimmers featuring $\mu_C \approx 0$ ⁴⁸.

V. COMPARISON WITH HYDRODYNAMIC INTERACTIONS

We now exploit the achieved explicit knowledge of the phoretic interaction coefficients for a comparison with hydrodynamic interactions.

Uniform surface mobility: Besides possible $1/r^2$ -contributions which may be led by a small coefficient and are discussed below, Janus swimmers always induce a $1/r^3$ flow field, which we now compare with phoretic interactions. The flow field induced by an isotropic (i.e. non-active) colloid in an imposed gradient at a point \mathbf{r} relative to its center and well beyond its interfacial layer reads⁵³ ($r := |\mathbf{r}|$; $\hat{\mathbf{r}} = \mathbf{r}/r$)

$$\mathbf{v}(\mathbf{r}) = \frac{1}{2} \left(\frac{R}{r} \right)^3 (3\hat{\mathbf{r}}\hat{\mathbf{r}} - I) \cdot \mathbf{v}_0 \quad (9)$$

The same flow field occurs for Janus colloids with a uniform surface mobility in a self-produced phoretic gradient, assumed that the colloids cannot distinguish between self-produced and imposed phoretic fields. Accordingly, this (and similar) flow fields commonly occur for Janus colloids (with a uniform surface mobility) in the literature^{20,28,54–60}. (Additional flow field contributions may of course arise if the boundary conditions are different than for a colloid in an imposed gradient⁶¹.) We estimate the relative strength of phoretic (7) and $1/r^3$ -hydrodynamic flows (9) advecting other colloids (in far field) via a parameter $m(r) := 8r^3 |\partial_r(\exp[-\kappa r]/r)| / (3R)$. Without a decay of the phoretic field ($\kappa = 0$)^{12,16,39,41} we have $m \gg 1$ at all relevant distances (i.e. beyond the near field regime) so that phoretic interactions should dominate. For $\kappa > 0$, hydrodynamic interactions may dominate at very long distances, but rather not at typical ones. For $R = 1\mu\text{m}$ colloids at 10% area fraction (average distance $5.6\mu\text{m}$) and $\kappa R = 0.25$, we find $m \sim 8.8$, and even for $\kappa R \sim 0.5$, we have $m \sim 3.5$; higher densities further support phoretic interactions. Hydrodynamic $1/r^3$ -interactions and phoretic interactions would break even at distances of $\sim 25R$ for $\kappa R = 0.25$ and at $\sim 10R$ for $\kappa R = 0.5$.

Nonuniform surface mobility: Janus swimmers with a non-uniform surface-mobility show additional $1/r^2$ force-dipole contributions^{9,63,64}, whose radial component scales as⁶⁴ $v(r) \sim |\mu_r|(R/r)^2 v_0$. Thus, for $\kappa = 0$, phoretic interactions should be $4/(3|\mu_r|)$ times stronger than hydrodynamic $1/r^2$ -interactions, at any distance. We roughly estimate $1/|\mu_r| \sim 3 - 20$ for commonly used coating materials⁵¹, so

that phoretic interactions seem to dominate. Differently, for Janus colloids with a strongly nonuniform surface mobility ($|\mu_r| \sim 1$), which might apply e.g. to certain electrophoretic swimmers with functionalized surfaces and to thermophoretic swimmers with thick caps⁴⁸ hydrodynamic interactions would be similarly strong as the isotropic component of phoretic interactions. If phoretic interactions are screened ($\kappa > 0$), a comparison of $v(r) \sim |\mu_r|(R/r)^2 v_0$ with Eq. (7) suggests that phoretic and hydrodynamic $1/r^2$ -interactions break even at a distance of $r \approx [-1 - W(-1, -3|\mu_r|/(4e))] / \kappa$ where $W(k, x)$ is the k -th branch of the Lambert W -function (product logarithm). Thus, e.g. for $|\mu_r| = 0.2$, phoretic interactions dominate up to a critical distance of about $3.4/\kappa \approx 13.5R$ for $\kappa R = 0.25$, or at area fractions $> 1.7\%$ in uniform suspensions.

Alignment and Isotropy: In addition to the pure strength-comparison discussed so far, we note the following: (i) Phoretic interactions receive additional support from the alignment contribution (at order $\partial_r[\exp(-\kappa r)/r]$), Eq. (8), which on its own can initiate structure formation even at very low density²⁹. These alignment contributions are particularly important when $|\mu_r|$ is large and might then dominate the collective behaviour of active colloids. (ii) Phoretic interactions are isotropic (in leading order) and hence superimpose even for randomly oriented particles, whereas anisotropic hydrodynamic flows might mutually cancel to some extent (in bulk). Possibly, this could additionally support phoretic interactions over hydrodynamic ones and might explain why simulations of spherical squirmers involving only hydrodynamic interactions do not show much structure formation at packing fractions below $\sim 30 - 40\%$ even for large $|\mu_r|$ ^{65,66}, whereas phoretic interactions yield structure formation even at very low density as well will see below. These findings are consistent with microscopic simulations of Janus colloids showing clustering at low density due to phoretic interactions, but not without²⁰. (This does of course not imply, that hydrodynamic interactions essentially average out; (rod-shaped) pushers for example are known to destabilize the isotropic phase, at least in the absence of rotational diffusion^{30,67}.)

Limitations: Conversely to the discussed cases, hydrodynamic far-field interactions should dominate over phoretic interactions for strong effective screening ($\alpha \gg 1$) and in suspensions at very low density ($\lesssim 1 - 2\%$ or so, depending on α as quantified above). Hydrodynamic interactions might also be comparatively important for significantly nonspherical Janus colloids and for strongly asymmetric coating geometries. Also in near field, which we do not discuss here, both hydrodynamic and phoretic interactions are comparatively involved of course. Finally, note that our comparison is based on a simple comparison of pairwise interaction strength, not accounting e.g. for a possible collective impact of momentum conservation due to the solvent; also our results apply to Janus colloids moving by a self-produced surface slip; in certain swimmers, e.g.^{23,62}, phoretic interactions might be more complicated.

VI. THE ACTIVE ATTRACTIVE ALIGNING MODEL

To describe the collective behaviour of N active colloids, we now consider the Active Brownian particle model as a standard minimal model for active colloids and use our previous results to additionally account for phoretic interactions. Using $x_u = R$ and $t_u = 1/D_r$ as space and time units, where D_r is the translational diffusion constant, and introducing the Péclet number $\text{Pe} = v_0/(D_r R)$ this model reads (in dimensionless units and for colloids moving in quasi-2D):

$$\dot{\mathbf{x}}_i = \text{Pe} \mathbf{p}_i + \mathbf{f}_s(\mathbf{x}_i); \quad \dot{\theta}_i = \sqrt{2}\eta_i(t) \quad (10)$$

Eqs. (10) describe particles which sterically repel each other (here represented by dimensionless forces \mathbf{f}_s preventing particles to overlap at short distances) and self-propel with a velocity v_0 in directions $\mathbf{p}_i = (\cos \theta_i, \sin \theta_i)$ ($i = 1..N$) which change due to rotational Brownian diffusion; here η_i represents Gaussian white noise with zero mean and unit variance. Following Eq. (7,8), we can now account for phoretic far-field interactions leading to the ‘‘Active Attractive Aligning Model’’, or AAA model. We define this model for colloids moving in quasi-2D and phoretic fields diffusing in 3D space (see below for a 3D variant and⁶⁹ for the possible impact of a lower substrate):

$$\begin{aligned} \dot{\mathbf{x}}_i &= \text{Pe} \mathbf{p}_i - \frac{4\text{Pe}v}{3} \nabla u + \mathbf{f}_s(\mathbf{x}_i) \\ \dot{\theta}_i &= \frac{3\text{Pe}\mu_r}{2} \mathbf{p}_i \times \nabla u + \sqrt{2}\eta_i(t) \end{aligned} \quad (11)$$

Here, $\nabla u = \sum_{j=1; j \neq i}^N \nabla_{\mathbf{x}_i} \frac{e^{-\alpha x_{ij}}}{x_{ij}}$ with $x_{ij} = |\mathbf{x}_i - \mathbf{x}_j|$ and $\mathbf{a} \times \mathbf{b} = a_1 b_2 - a_2 b_1$ for 2D vectors \mathbf{a}, \mathbf{b} and where we have introduced a screening number $\alpha = R\sqrt{k_d/D_c}$. Remarkably, since we have $v = \pm 1$, and expect in many cases $|\mu_r| \ll 1$ ⁵¹, for a given screening number α (realistic values might be $\alpha \sim 0.25 - 0.65$, Fig. 1G), the strength of phoretic interactions is mainly controlled by one genuine parameter - the Péclet number. In our simple derivation, we have identified phoretic translations and rotations of the colloids with formally identical expressions representing reciprocal interaction forces (attractive Yukawa interactions for $v = -1$; Coulomb for $\alpha = 0$) and (nonreciprocal) torques aligning the self-propulsion direction of the colloids, towards ($\mu_r > 0$, positive taxis) or away ($\mu_r < 0$, negative taxis) from regions of high particle density. The AAA model can be viewed as a description of active colloids containing interactions in leading order in μ_r (if $|\mu_r| \ll 1$) *individually* for the center of mass and the orientational dynamics.

VII. PROPERTIES OF THE AAA MODEL

(i) For $\mu_r = 0, v = -1$; the AAA model reduces to active Brownian particles with isotropic attractions; however, as opposed to corresponding phenomenological models^{71–75,84}, the AAA model explicitly relates the interaction strength to the Péclet number. Setting $v \rightarrow 0$ instead, links the AAA

model with the Phoretic Brownian particle model²⁹ which focuses on phoretic alignment contributions for simplicity, but tracks the time-evolution of the phoretic field explicitly.²⁹ (ii) The AAA model is based on the assumption that the phoretic fields relax quasi-instantaneously to their steady state. When they relax slower, which can happen even for very large D_c ²⁹, the phoretic field cannot be eliminated and the AAA model becomes invalid; presumably this is relevant mainly for repulsive phoretic interactions ($v = 1$ or $\mu_r < 0$)²⁹. (iii) The Yukawa interactions in Eqs. (11) are reciprocal only when considering identical colloids. Mixtures of nonidentical Janus colloids, active-passive mixtures or of uniformly coated colloids lead to nonreciprocal interactions inducing a net motion of pairs^{18,45,76}. For example, passive particles can be included in the AAA model via $\dot{\mathbf{x}}_i^{\text{passive}} = -(4/3)\mu v \text{Pe} \nabla u$ where Pe is the Péclet number of the active colloids and $\mu = 2\mu_p/(\mu_N + \mu_C)$ with μ_p being the surface mobility of the (isotropic) passive colloid. (iv) For single-species isotropically coated colloids ($v_0 = 0$) the AAA model reduces to the hard-core Yukawa model (when accounting for translational diffusion). Thus, chemically active colloids can be used to realize the (attractive or repulsive) hard-core Yukawa model, which has been widely used to describe effective interactions between charged colloids^{77,78}, globular proteins⁷⁹ and fullerenes⁸⁰. (v) Generalizations of the AAA model to 3D are straightforward; here the orientational dynamics follows $\dot{\mathbf{p}}_i = (3/2)\text{Pe}\mu_r (I - \mathbf{p}_i \mathbf{p}_i) \nabla u + \sqrt{2}\boldsymbol{\eta}_i \times \mathbf{p}_i$ where \mathbf{p}_i is the 3D unit vector representing the swimming direction of particle i , $\boldsymbol{\eta}_i$ represents Gaussian white noise of zero mean and unit variance and \times now represents the standard 3D cross product.

VIII. DYNAMIC CLUSTERING IN THE AAA MODEL

The AAA model generically leads to dynamic clustering at low density. We exemplarily show this in Brownian dynamics simulations (Fig. 1), at $\text{Pe} = 100$ and $\alpha = 0.25$, where we truncate the Yukawa interactions at 16 particle radii: (i) Without alignment ($\mu_r = 0$) clusters dynamically emerge, break up and move through space, similar as in canonical experiments^{12,22–24} (see Movie 1). For an area fraction of $\phi = 5\%$, these clusters do not grow beyond a certain size (red line in Fig. 1 F). Conversely, for $\phi = 10\%$ (Movie 2) once a cluster has reached a certain size (Fig. 1 B), it continues growing for a comparatively long time (panel E, green line). However, also here, the clusters eventually stop growing (at a non-macroscopic size) and dynamically break up leading again to a finite average cluster size (Movie 2). Thus, screened phoretic attractions and active diffusion are sufficient to generate dynamic clusters, although phoretic- and other near-field interactions, all neglected here, would of course modify the properties of the clusters, once they have emerged. (ii) Similarly for $\mu_r = -1$ (strong negative taxis) we also find dynamic clusters (panel C); here negative taxis stabilizes the dynamic cluster phase and clusters do not grow at late times for $\phi = 0.1$ (black curve in F) and also not for $\phi = 0.2$ (not shown). This combination of attractive translation combined with negative taxis resembles⁴⁰. (iii) For $\mu_r = 1$ (strong positive taxis) we find

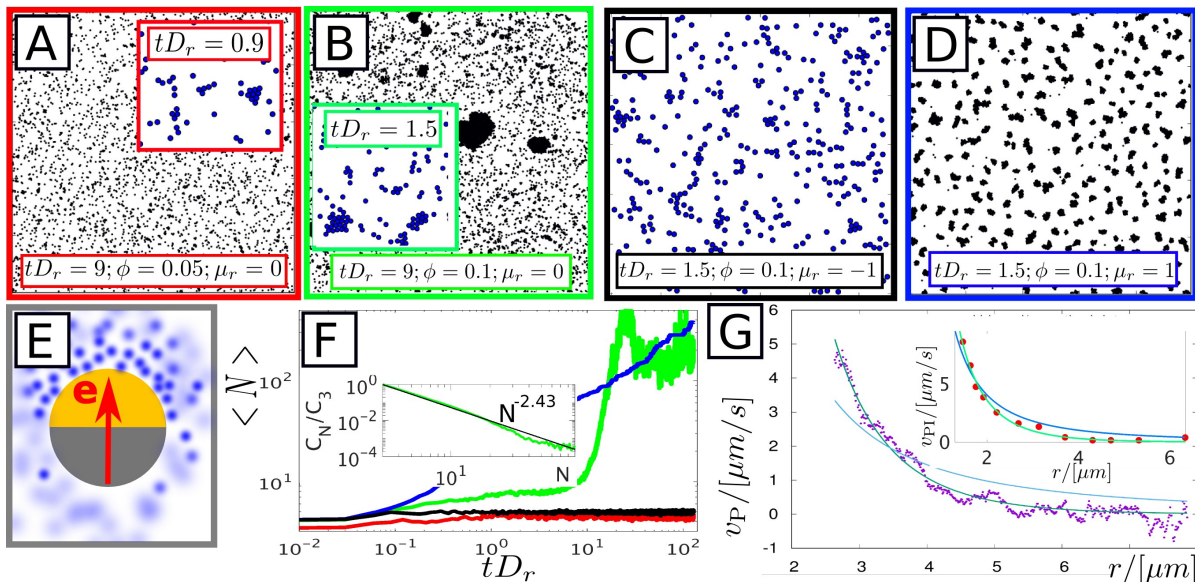


FIG. 1. A-D: Dynamic Clustering in the AAA model; snapshots from Brownian dynamics simulations for $N = 400 - 8000$ with $Pe = 100$, $\alpha = 0.25$, $v = -1$ at area fractions and times given in the key. Panels A-C show dynamic clusters which continuously emerge and split up; yielding a finite (nonmacroscopic) cluster size in A,C at late times; D shows the system on the way to a ‘chemotactic collapse’. E: Schematic of a Janus colloid swimming with its catalytic cap ahead, hence interacting attractively with other colloids ($v = -1$). F: Time-evolution of the mean cluster size calculated by applying a grid with spacing $2x_u$ and counting connected regions; colors refer to frames in A-D. Inset: Time-averaged cluster size distribution for the data of panel B (green) and fit (black) indicating an algebraic decay at small N ; C_N/C_3 is the ratio of N -particle clusters to 3-particle clusters. G: Velocity of passive tracers due to the phoretic field produced by Janus colloids in experiments¹⁶ (main figure, dots show our own averages over tracer trajectories) and¹² (inset; dots are based on Fig. 2B in¹²). Green and blue curves show fits with and without effective screening respectively. The fits allow for an (upper) estimate of $\alpha \lesssim (0.25 - 0.65)$ in both cases and suggest $|\mu| = 2\mu_P/(\mu_N + \mu_C) \sim 2 - 3$ for¹² and $|\mu| \gtrsim 5$ for¹⁶, which may however be influenced by additional short-range interactions.

rigid clusters (panel D) which coalesce and form one macro-cluster at late times (not shown).

Note that the clusters seen in cases (i),(ii) differ from those occurring as a precursor of motility-induced phase separation^{23,26,81–86} in the (repulsive) Active Brownian particle (ABP) model^{23,26,81–86}. The ABP model only leads to very small and short lived clusters at low area fractions; here the cluster size distribution decays exponentially with the number of particles in the cluster (unless we are at area fractions of $\gtrsim 30\%$ close to the transition to motility induced phase separation). In contrast, both in experiments²⁴ and in the AAA model, we see significant clusters at low area fractions ($\leq 10\%$), with a cluster size distribution which decays algebraically at small sizes if the overall area fraction is not too low (inset in panel F). A detailed comparison of cluster sizes and distributions with experiments may be performed in future works, but might require to account for factors beyond the minimal AAA model, such as phoretic and other near-field interactions, a 3D modeling accounting explicitly for a confinement and an understanding of the dependence of κ on v_0 .

IX. CONCLUSIONS

The derived AAA model provides a minimal description of autophoretic active colloids including phoretic far-field in-

teractions, whose strength we explicitly determine. Consequences of our results are as follows: (i) The AAA model naturally leads to dynamic clustering in the same parameter regime as canonical experiments with active colloids. This suggests that dynamic clustering can occur as a generic result of the interplay of screened phoretic attractions and active diffusion. (ii) Phoretic interactions are of crucial importance in typical active colloids. In a broad class of autophoretic Janus colloids (half-capped, uniform or moderately nonuniform surface mobility) and corresponding active-passive mixtures, they even seem to dominate over the more commonly considered hydrodynamic interactions. Conversely, hydrodynamic interactions probably dominate over screened phoretic interactions at very low density ($\lesssim 1 - 2\%$ area fraction, depending on α) and for cases of strong effective screening ($\alpha \gg 1$). Finally, for Janus colloids with a strongly asymmetric coating geometry or a strongly nonuniform surface mobility (e.g. thermophoretic swimmers with thick caps), phoretic interactions and hydrodynamic interactions may be similarly strong. Note also that in certain swimmers^{23,62}, phoretic interactions might be more complicated than described here. Future generalizations could account for anisotropy and near-field effects and could explicitly account for both hydrodynamic and phoretic interactions to obtain a more general, yet probably more complicated description of active colloids.

Acknowledgements We thank Frederik Hauke for making Fig. 1G (main panel) available and Mihail Popescu and

Siegfried Dietrich for useful discussions.

- 1 W. F. Paxton, K. C. Kistler, C. C. Olmeda, A. Sen, S. K. St. Angelo, Y. Cao, T. E. Mallouk, P. E. Lammert, and V. H. Crespi, *J. Am. Chem. Soc.* **126**, 13424 (2004).
- 2 J. R. Howse, R. A. Jones, A. J. Ryan, T. Gough, R. Vafabakhsh, and R. Golestanian, *Phys. Rev. Lett.* **99**, 048102 (2007).
- 3 C. Bechinger, R. Di Leonardo, H. Löwen, C. Reichhardt, G. Volpe, and G. Volpe, *Rev. Mod. Phys.* **88**, 045006 (2016).
- 4 M. N. Popescu, W. E. Uspal, and S. Dietrich, *Eur. Phys. J. Spec. Top.* **225**, 2189 (2016).
- 5 J. L. Moran and J. D. Posner, *Ann. Rev. Fluid Mech.* **49**, 511 (2017).
- 6 T. R. Kline, W. F. Paxton, T. E. Mallouk, and A. Sen, *Angew. Chem. Int. Ed.* **44**, 744 (2005).
- 7 R. Golestanian, T. B. Liverpool, and A. Ajdari, *New J. Phys.* **9**, 126 (2007).
- 8 H.-R. Jiang, N. Yoshinaga, and M. Sano, *Phys. Rev. Lett.* **105**, 268302 (2010).
- 9 S. J. Ebbens and D. A. Gregory, *Acc. Chem. Res.* (2018).
- 10 X. Ma, K. Hahn, and S. Sanchez, *J. Am. Chem. Soc.* **137**, 4976 (2015).
- 11 A. F. Demirörs, M. T. Akan, E. Poloni, and A. R. Studart, *Soft Matter* **14**, 4741 (2018).
- 12 J. Palacci, S. Sacanna, A. P. Steinberg, D. J. Pine, and P. M. Chaikin, *Science* **339**, 936 (2013).
- 13 S. H. Klapp, *Curr. Opin. Colloid Interface Sci.* **21**, 76 (2016).
- 14 C. Maggi, J. Simmchen, F. Saglimbeni, J. Katuri, M. Dipalo, F. De Angelis, S. Sanchez, and R. Di Leonardo, *Small* **12**, 446 (2016).
- 15 J. Zhang, J. Yan, and S. Granick, *Angew. Chem. Int. Ed.* **55**, 5166 (2016).
- 16 D. P. Singh, U. Choudhury, P. Fischer, and A. G. Mark, *Adv. Mater.* **29** (2017).
- 17 H. R. Vutukuri, B. Bet, R. Roij, M. Dijkstra, and W. T. Huck, *Sci. Rep.* **7**, 16758 (2017).
- 18 F. Schmidt, B. Liebchen, H. Löwen, and G. Volpe, arXiv preprint arXiv:1801.06868 (2018).
- 19 A. Aubret, M. Youssef, S. Sacanna, and J. Palacci, *Nat. Phys.* (2018).
- 20 M.-J. Huang, J. Schofield, and R. Kapral, *New J. Phys.* **19**, 125003 (2017).
- 21 P. H. Colberg, and R. Kapral, *J. Chem. Phys.* **147**, 064910 (2017).
- 22 I. Theurkauff, C. Cottin-Bizonne, J. Palacci, C. Ybert, and L. Bocquet, *Phys. Rev. Lett.* **108**, 268303 (2012).
- 23 I. Buttinoni, J. Bialké, F. Kümmel, H. Löwen, C. Bechinger, and T. Speck, *Phys. Rev. Lett.* **110**, 238301 (2013).
- 24 F. Ginot, I. Theurkauff, F. Detcheverry, C. Ybert, and C. Cottin-Bizonne, *Nat. Comm.* **9**, 696 (2018).
- 25 P. Romanczuk, M. Bär, W. Ebeling, B. Lindner, and L. Schimansky-Geier, *Eur. Phys. J.* **202**, 1 (2012).
- 26 M. E. Cates and J. Tailleur, *Annu. Rev. Condens. Matter Phys.* **6**, 219 (2015).
- 27 J. Elgeti, R. G. Winkler, and G. Gompper, *Rep. Prog. Phys.* **78**, 056601 (2015).
- 28 A. Zöttl and H. Stark, *J. Phys. Cond. Matter* **28**, 253001 (2016).
- 29 B. Liebchen, D. Marenduzzo, and M. E. Cates, *Phys. Rev. Lett.* **118**, 268001 (2017).
- 30 D. Saintillan and M. J. Shelley, *Phys. Rev. Lett.* **100**, 178103 (2008).
- 31 J. S. Guasto, K. A. Johnson, and J. P. Gollub, *Phys. Rev. Lett.* **105**, 168102 (2010).
- 32 K. Drescher, R. E. Goldstein, N. Michel, M. Polin, and I. Tuval, *Phys. Rev. Lett.* **105**, 168101 (2010).
- 33 S. Heidenreich, J. Dunkel, S. H. Klapp, and M. Bär, *Phys. Rev. E (R)* **94**, 020601 (2016).
- 34 U. B. Kaupp and L. Alvarez, *Eur. Phys. J. Spec. Top.* **225**, 2119 (2016).
- 35 R. Jeanneret, M. Contino, and M. Polin, *Eur. Phys. J. Spec. Top.* **225**, 2141 (2016).
- 36 J. Stenhammar, C. Nardini, R. W. Nash, D. Marenduzzo, and A. Morozov, *Phys. Rev. Lett.* **119**, 028005 (2017).
- 37 A. Daddi-Moussa-Ider, M. Lisicki, A. J. Mathijssen, C. Hoell, S. Goh, J. Bławdziewicz, A. M. Menzel, and H. Löwen, *J. Phys. Cond. Matter* **30**, 254004 (2018).
- 38 T. Vissers, A. T. Brown, N. Koumakis, A. Dawson, M. Hermes, J. Schwarz-Linek, A. B. Schofield, J. M. French, V. Koutsos, J. Arlt, et al., *Sci. Adv.* **4**, eaao1170 (2018).
- 39 S. Saha, R. Golestanian, and S. Ramaswamy, *Phys. Rev. E* **89**, 062316 (2014).
- 40 O. Pohl and H. Stark, *Phys. Rev. Lett.* **112**, 238303 (2014).
- 41 M. Meyer, L. Schimansky-Geier, and P. Romanczuk, *Phys. Rev. E* **89**, 022711 (2014).
- 42 B. Liebchen, D. Marenduzzo, I. Pagonabarraga, and M. E. Cates, *Phys. Rev. Lett.* **115**, 258301 (2015).
- 43 B. Liebchen, M. E. Cates, and D. Marenduzzo, *Soft Matter* **12**, 7259 (2016).
- 44 M. Nejad and A. Najafi, arXiv preprint arXiv:1712.06004 (2018).
- 45 R. Soto and R. Golestanian, *Phys. Rev. Lett.* **112**, 068301 (2014).
- 46 S. Gonzalez and R. Soto, *New J. Phys.* **20**, 053014 (2018).
- 47 J. L. Anderson, *Ann. Rev. Fluid Mech.* **21**, 61 (1989).
- 48 T. Bickel, G. Zecua, and A. Würger, *Phys. Rev. E(R)* **89**, 050303 (2014).
- 49 For self-diffusiophoretic swimmers we understand c as the sum of fuel and reaction-product species and D_c as an effective diffusion coefficient of the combined field.
- 50 Self-thermophoretic swimmers lead to an almost identical expression for the self-propulsion velocity, differing only by a constant, e.g. $2/3$, depending on the 'field deformation factor'⁴⁸.
- 51 Consider a solute of neutral, dipolar molecules (water, H_2O_2) featuring excluded volume and dipolar interactions with a colloidal surface. Excluded volume interactions should not depend much on the surface material⁴⁷ favoring $\mu_r = 0$ for Janus particles. The surface mobility of a colloid due to dipolar interactions reads⁴⁷ $\mu \approx \frac{-16kT}{3\eta} \left(\frac{\mu_D}{Ze} \right)^2 \xi^2 + \mathcal{O}(\xi^4)$ where $\xi = \tanh[Ze\zeta/(4kT)]$ with ζ being the zeta potential, μ_D the solute dipole moment and Z the valence of the support electrolyte (we assume $Z = 1$; $Z > 1$ reduces $|\mu_r|$). Applying these expressions to the halves of a Janus colloids with cap (C) and neutral side (N) then suggests $|\mu_r| = |(\mu_C - \mu_N)/(\mu_C + \mu_N)| \approx |(\xi_C^2 - \xi_N^2)/(\xi_C^2 + \xi_N^2)|$. Measurements for typical coating materials: $\zeta \approx -64mV$ both for isotropic $2R = 1.7\mu m$ polystyrene (PS) and $1\mu m$ gold spheres in $5\%H_2O_2$ solution⁸⁷; $\zeta \sim -52mV, -67mV$ for polystyrene and silica colloids (sizes $1 - 3\mu m$) respectively in $0.01M KCl$ solution¹⁰ and for $2R = 1\mu m$ spheres in water $\zeta \sim -50mV$ (PS, SiO_2), and $\zeta \sim -63mV$ (TiO_2)⁸⁸. Measurements for the two halves of a $2R = 4.8\mu m$ PS-Pt Janus colloid in water (and in $5\%, 10\%H_2O_2$) yield $\zeta \sim -95mV$ ($-105mV, -110mV$) for the PS side and $\zeta \sim -80mV$ ($-70mV, -70mV$) for the Pt⁸⁹. Based on these values we estimate $|\mu_r| \sim 0.05 - 0.3$ for typical Janus swimmers (or less if excluded volume interactions dominate). Similarly, for electrophoretic Janus swimmers $|\mu_r| \sim |(\xi_C - \xi_N)/(\xi_C + \xi_N)|$ and is therefore significantly smaller than 1 for most typical material combinations.
- 52 Instabilities for chemorepulsive colloids at $k_d = 0, |\mu_r| = 1$ occur at about $Pe > 5$ and area fractions $\sim 10\%$, based on phoretic alignment interactions alone (see the $k_d = 0, |\mu_r| = 1$ -phase diagram in²⁹); when e.g. $|\mu_r| = 0.2$, they would still occur for typical Janus colloids with $Pe > 25$, unless effective screening is strong.
- 53 F. Morrison Jr, *J. Colloid Interface Sci.* **34**, 210 (1970).
- 54 F. Jülicher and J. Prost, *Eur. Phys. J. E* **29**, 27 (2009).
- 55 T. Bickel, A. Majee, and A. Würger, *Phys. Rev. E* **88**, 012301 (2013).
- 56 M. Yang and M. Ripoll, *Soft Matter* **9**, 4661 (2013).
- 57 M. Yang, A. Wysocki, and M. Ripoll, *Soft Matter* **10**, 6208 (2014).
- 58 D. A. Fedosov, A. Sengupta, and G. Gompper, *Soft Matter* **11**, 6703 (2015).
- 59 P. Bayati and A. Najafi, *J. Chem. Phys.* **144**, 134901 (2016).
- 60 P. Kreissl, C. Holm, and J. De Graaf, *J. Chem. Phys.* **144**, 204902 (2016).
- 61 S. Y. Reigh, M.-J. Huang, J. Schofield, and R. Kapral, *Phil. Trans. R. Soc.* **374**, 20160140 (2016).
- 62 J.-R. Gomez-Solano, S. Samin, C. Lozano, P. Ruedas-Batuceas, R. van Roij, and C. Bechinger, *Sci. Rep.* **7**, 14891 (2017).
- 63 Y. Ibrahim and T. B. Liverpool, *Eur. Phys. J. Spec. Top.* **225**, 1843 (2016).
- 64 M. N. Popescu, W. E. Uspal, Z. Eskandari, M. Tasinkevych, and S. Dietrich, *Eur. Phys. J. E* **41**, 145 (2018).
- 65 A. Zöttl and H. Stark, *Phys. Rev. Lett.* **112**, 118101 (2014).
- 66 J. Blaschke, M. Maurer, K. Menon, A. Zöttl, and H. Stark, *Soft Matter* **12**, 9821 (2016).
- 67 D. Saintillan and M. J. Shelley, *Phys. Rev. Fluids* **20**, 123304 (2008).
- 68 N. Yoshinaga and T. B. Liverpool, *Phys. Rev. E* **96**, 020603 (2017).
- 69 If a lower substrate is present which fully 'reflects' the phoretic field, this can be accounted for by mirror sources, resulting in an additional factor of 2 for the strength of phoretic interactions in far-field.

- ⁷⁰G. S. Redner, A. Baskaran, and M. F. Hagan, *Phys. Rev. E* **88**, 012305 (2013).
- ⁷¹B. M. Mognetti, A. Šarić, and S. Angioletti-Uberti, A. Cacciuto, C. Valeriani, D. Frenkel, *Phys. Rev. Lett.* **111**, 245702 (2013).
- ⁷²V. Prymidis, H. Sielcken, and L. Filion, *Soft Matter* **11**, 4158 (2015).
- ⁷³M. Rein and T. Speck, *Eur. Phys. J. E* **39**, 84 (2016).
- ⁷⁴F. Alarcón, C. Valeriani, and I. Pagonabarraga, *Soft Matter* **13**, 814 (2017).
- ⁷⁵T. Bäuerle, A. Fischer, T. Speck, and C. Bechinger, *Nat. Comm.* **9**, 3232 (2018).
- ⁷⁶L. Wang, M. N. Popescu, F. L. Stavale, A. Ali, T. Gemming, and J. Simmchen, *Soft Matter* (2018).
- ⁷⁷A.-P. Hynninen and M. Dijkstra, *J. Phys. Cond. Matter* **15**, S3557 (2003).
- ⁷⁸M. Heinen, A. J. Banchio, and G. Nägele, *J. Chem. Phys.* **135**, 154504 (2011).
- ⁷⁹E. Schöll-Paschinger, N. E. Valadez-Pérez, A. L. Benavides, and R. Castañeda-Priego, *J. Chem. Phys.* **139**, 184902 (2013).
- ⁸⁰J.-X. Sun, *Phys. Rev. B* **75**, 035424 (2007).
- ⁸¹J. Tailleur and M. Cates, *Phys. Rev. Lett.* **100**, 218103 (2008).
- ⁸²Y. Fily and M. C. Marchetti, *Phys. Rev. Lett.* **108**, 235702 (2012).
- ⁸³J. Bialké, H. Löwen, and T. Speck, *Europhys. Lett.* **103**, 30008 (2013).
- ⁸⁴G. S. Redner, M. F. Hagan, and A. Baskaran, *Phys. Rev. Lett.* **110**, 055701 (2013).
- ⁸⁵J. Stenhammar, A. Tiribocchi, R. J. Allen, D. Marenduzzo, and M. E. Cates, *Phys. Rev. Lett.* **111**, 145702 (2013).
- ⁸⁶D. Levis, J. Codina, and I. Pagonabarraga, *Soft Matter* **13**, 8113 (2017).
- ⁸⁷W. Wang, W. Duan, A. Sen, and T. E. Mallouk, *Proc. Natl. Acad. Sci.* p. 201311543 (2013).
- ⁸⁸S. Ni, E. Marini, I. Buttinoni, H. Wolf, and L. Isa, *Soft Matter* **13**, 4252 (2017).
- ⁸⁹S. Das, G. Astha, A.I. Campbell, J. Howse, A. Sen, D. Velegol, R. Golestanian, and S.J. Ebbens, *Nat. Comm.* **6**, 8999 (2015).